Transactions of the TSME (2019) Vol.7, No. 1, 1-10
Journal of Research and Applications in Mechanical Engineering

ISSN 2229-2152 print
DOI: 10.14456/jrame.2019.1

Research Article

THERMAL CHARACTERIZATION IN CIRCULAR TUBE INSERTED WITH DIAMOND-SHAPED RINGS

P. Promthaisong [1]
S. Skullong [2,*]
[1] *Department of Mechanical Engineering, Faculty of Engineering, Mahanakorn University of Technology, Bangkok 10530, Thailand*
[2] *Department of Mechanical Engineering, Faculty of Engineering at Sriracha, Kasetsart University Sriracha Campus, 199 M.6, Sukhumvit Rd., Sriracha, Chonburi 20230, Thailand*

Received 24 February 2019
Revised 7 May 2019
Accepted 10 May 2019

ABSTRACT:
The article presents the influence of diamond-shaped rings (DRs) mounted repeatedly in a uniform heat-fluxed heat exchanger tube on flow resistance and thermal behaviors. In the current study, the DR elements used for producing the longitudinal vortex flows were placed in the tube by employing two small rods to connect the DRs together. Effects of three relative ring-pitches or pitch ratios (R_P = P/D = 0.5, 1.0, 2.0) and three ring blockage ratios (R_B = b/D = 0.1, 0.15 and 0.2) at the attack angle of 45° on Nusselt number (Nu), friction factor (f) and thermal enhancement factor (TEF) in turbulence regimes, Reynolds number (Re) between 4220–25,800 are examined. The results have shown that the heat transfer and pressure loss increase considerably with raising R_B but with the decline of R_P. The maximum Nu and f obtained at R_B = 0.2 and R_P = 0.5 are, respectively, about 3.21–4.18 and 11.73–32.85 times above the smooth tube. The highest TEF around 1.57 is seen at R_B = 0.10 and R_P = 1.0. Furthermore, empirical correlations for Nu, f and TEF were established and found to fit the experimental data with deviations within ±8%, ±9% and ±5%, respectively.

Keywords: *Diamond rings, Heat exchanger, Vortex generators, Thermal performance*

1. INTRODUCTION

Heat transfer enhancement (HTE) techniques have been utilized extensively in many engineering applications and industries for example, aerospace, air conditioner, automotive, refrigerators, heat exchanger, etc. For decades, many researchers have investigated the utilization of swirl/vortex generator devices in enhancing the rate of heat transfer in heat exchanger tubes fitted with various insert-types of swirl/vortex generators. Vortex generators (VGs) are devices for producing swirl/vortex flows like twisted tape [1], coiled wire [2], wing [3], winglet [4, 5], and vortex rings [6, 7], and are regarded as an important passive HTE technique to save energy, without adding more energy input. Those devices are designed and used to reduce the size and the production cost of a compact heat exchanger and also to upgrade the existing tubular heat exchanger for a retrofit. Owing to low cost, convenient disassembly and easy maintenance, VGs being used as the tube insert have been extensively applied in the improvement of heat exchangers.

For continuous vortex-flow devices, wire coils and twisted tapes have been extensively applied for enhancing the heat transfer rate in a tubular heat exchanger. Promvonge [8] studied the enhancement of thermal performance by using coiled square wire inserts and found that the wire coils performed much better than the plain tube alone.

* Corresponding author: Sompol Skullong
E-mail address: sfengsps@src.ku.ac.th, sompol@eng.src.ku.ac.th

Chiu and Jang [9] investigated the thermohydraulic characteristics in a round tube with different inserts such as longitudinal-strips with/without holes and twisted-tapes with three twist angles (α = 15.3°–34.3°). Promvonge et al. [10] examined experimentally the effect of twist ratio on heat transfer and friction behaviors in a helical-ribbed tube with double twisted tapes. Hong et al. [11] proposed thermal behaviors of overlapped multiple twisted-tapes for Re ranging from 5800 to 19,200 and found that the triple twisted-tapes provided the highest thermal performance. The effects of alternation of clockwise and counterclockwise twisted tapes (ACCT tape) on thermal performance in a single-phase dual-pipe heat exchanger for Re = 3000 to 9000 were investigated by Man et al. [12].

Also, the decaying vortex/swirl-flow devices have been widely used in many heat exchanger tubes. Thermal performance behaviors in a round tube equipped with circular-ring turbulator (CRT) of different diameter ratios (DR) were reported by Kongkaitpaiboon et al. [13]. The best thermal performance was varied between 0.65 and 1.07 for using the CRT with DR=0.7 and PR=6. The influence of inclined horseshoe baffles at various baffle-pitch ratios (PR) and blockage ratios (BR) on flow resistance and thermal characteristics in a circular tube was investigated by Promvonge et al. [14] and the highest thermal performance was achieved for the baffles with P_R = 0.5 and B_R = 0.1. An experimental and numerical study on the thermal behaviors in a heat exchanger tube with punched-curved-winglet tape (P-CWT) as vortex generators was performed by Skullong et al. [15]. They found that the P-CWT at B_R = 0.1, P_R = 1.0 and hole diameter = 1.5 mm possessed the best thermal performance.

In the above literature review, the maximum thermal performance of the VG devices is approximately 1.5, for using wings/winglets/vortex rings, somewhat higher than that of the continuous vortex-flow devices found in the literature. A summary of previous researches on the performance enhancement in a tubular heat exchanger has shown that there were no data on heat transfer, friction factor and thermal performance in any heat exchanger tube fitted with vortex rings in the form of diamond-shaped rings (DR) in turbulent flows. In this paper, a new type of VG device by cutting and drilling to shape the diamond hole on the ring sheet was mounted periodically in the test tube. This is much fruitful in designing and upgrading the heat exchangers. So, the purpose of this work is divided into two aspects: (i) to investigate the heat transfer augmentation as well as the friction loss in a heat exchanger tube inserted with DRs at different size/arrangement in the form of R_B and R_P values, (ii) to give reliable correlations based on the experimental data of Nusselt number (Nu) and friction factor (f) and thermal enhancement factor (TEF).

2. EXPERIMENTATION

Figure 1 presents the schematic diagram and geometric parameters of the experimental facility. The experimental facility consisted of an inlet section (for fully developed flow), test section, exit section, supplied air and heating systems. In the test apparatus, the 2-mm thick (t) copper tube having a 50.8-mm inner-diameter (D) was totally 3000-mm long, included the 1200-mm test tube length (L) and the 200-mm exit-section whereas the 1600-mm inlet-section was adopted to become a fully-developed flow as it enters the test tube. In the test runs, air was flowed through the tube to obtain Re in a range of 4220 to 25800. An electric wire was coiled around the tube to achieve a uniform heat-flux tube wall (q'' = 600 W/m^2) while the electric power fed to the heating wire was regulated by a variac (AC power supply). To reduce the convection loss to the surrounding air, the ceramic insulations was applied to the outermost of the test tube.

A 2.2-kW high-pressure blower was employed to produce the room air (25 °C) to the tube system. Air flowed into an orifice-typed flowmeter mounted between the blower and the settling tank to measure the volume airflow rate at which the pressure drop of the flowmeter was measured by U-tube/inclined manometers. The varied airflow rate in the tube was done by regulating the speed of the blower-motor via an inverter. Two Resistance Temperature Detectors (RTD, Pt-100) were employed to measure the air inlet and exit temperatures while the surface temperatures were monitored by twenty-four thermocouples (T-type) located equally on the top and side walls of the tube. Whenever, temperatures of the outlet air and surfaces were unchanged around half an hour implying that it was in a steady state, all temperatures were collected via a data logger (Fluke 2680A). The pressure drop in the test tube was measured by a Dwyer (475-1-FM 475 Mark III) digital manometer. According to the methodology introduced by references [16], the uncertainties in measurements of temperature, velocity and pressure were, respectively, less than ±0.3%, ±4% and ±3%. The maximum uncertainties in other instruments were within ±1.2% for the flowmeter and ±1.1% for the manometer while the dimensionless parameters had the uncertainties around

3.5% for Nu, 6.8% for f and 3.2% for Re. More details of the experimental uncertainty calculation can be seen in Refs. [17].

The details and layouts on the investigation of 45º DRs are presented in Fig. 2. Aluminum strips with thickness (t) of 3 mm were used to form the diamond-shaped rings in the current work. The DR had a size of 50-mm width by 70-mm height (see Fig. 2) and mounted repeatedly in the tube with three blockage ratios ($R_B=e/D$= 0.1, 0.15 and 0.2) and pitch ratios ($R_P=P/D$=0.5, 1 and 2). The DR elements were linked together with two straight slim-rods attached tightly on their side-edges using superglue as seen in Fig. 2.

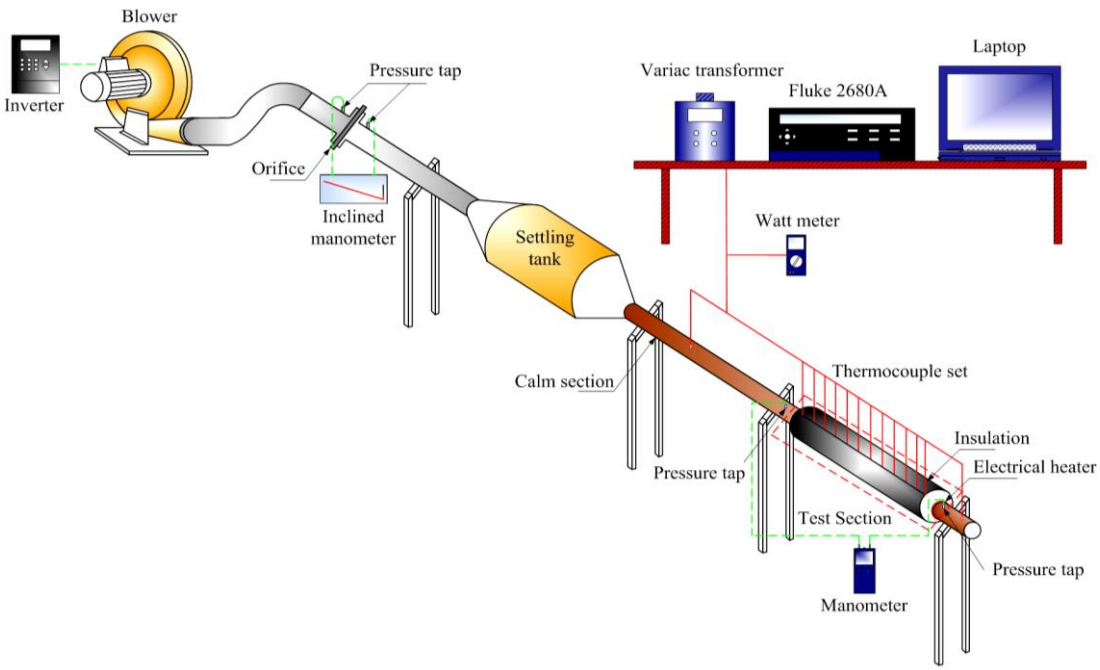

Fig. 1. Schematic sketch of experimental system.

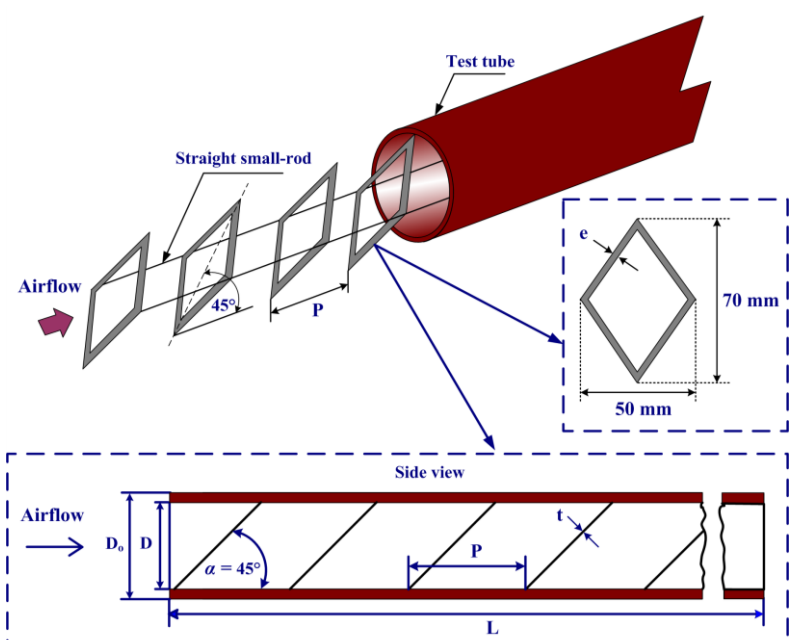

Fig. 2. Test tube inserted with 45° DR elements.

3. THEORETICAL ANALYSIS

The current work is carried out to investigate the heat transfer rate (Nusselt number, Nu), friction loss (friction factor, *f*), flow parameter (Reynolds number, Re) and thermal performance (thermal enhancement factor, TEF) in a tubular heat exchanger with DR inserts.

In this experiment, when air enters the test-duct at a steady flow, the heat transfer from the tube to air can be prescribed as:

$$Q_{\mathrm{a}} = \dot{m}C_{\mathrm{p,a}}\left(T_{\mathrm{o}} - T_{\mathrm{i}}\right) = VI - Q_{\mathrm{loss}}$$

where Q_{loss} is the tube convection heat loss to the surrounding air. With regard to a thermal resistance network for the cylindrical layer concept [18], the Q_{loss} can be written as:

$$Q_{\mathrm{loss}} = (T_{\mathrm{w}} - T_{\infty}) \Big/ \frac{\ln(r_{\mathrm{o}}/r_{\mathrm{i}})}{2\pi Lk} + \frac{1}{2\pi Lr_{\mathrm{o}}h_{\mathrm{o}}}$$

where h_{o}, T_{w}, T_{∞} are respectively, free convection coefficient of air between the outer insulation and the surrounding, local wall temperature along the tube, temperature of surrounding, while k, r_{i}, r_{o}, are respectively, insulation thermal conductivity, inner and outer radii of the tube.

For thermal equilibrium, Q_{loss} is found below 4% of the input power VI, supplied by the electrical wire. Due to air flowing steadily through the test tube, the heat transfer rate is equal to the convection heat and given by

$$Q_{\mathrm{a}} = Q_{\mathrm{conv}} \tag{1}$$

The convection heat transfer in the duct is calculated by

$$Q_{\mathrm{conv}} = hA\left(\tilde{T}_{\mathrm{w}} - T_{\mathrm{b}}\right) \tag{2}$$

in which

$$T_{\mathrm{b}} = (T_{\mathrm{o}} + T_{\mathrm{i}})/2 \tag{3}$$

and

$$\tilde{T}_{\mathrm{w}} = \sum T_{\mathrm{w}}/24 \tag{4}$$

The mean wall temperature, $\tilde{T}_{\mathrm{w}}$, is evaluated from 24 points of the wall temperatures lined equally along the tube. The average heat transfer coefficient (*h*) and Nusselt number (Nu) are written as

$$h = \dot{m}C_{\mathrm{p,a}}\left(T_{\mathrm{o}} - T_{\mathrm{i}}\right) / A\left(\tilde{T}_{\mathrm{w}} - T_{\mathrm{b}}\right) \tag{5}$$

where, *A* is the heat transfer surface area inside the tube, and determined by

$$A = \pi D_{\mathrm{i}} L \tag{6}$$

in which D_{i} is inner diameter of the tube.
The average Nu is calculated from the heat transfer coefficient (*h*) using the following relations:

$$\mathrm{Nu} = hD/k \tag{7}$$

The flow in terms of Reynolds numbers (Re) is evaluated by

$$\mathrm{Re} = UD/\nu \tag{8}$$

The friction factor (f) is estimated from pressure drop (ΔP) by its definition as

$$f = \frac{2}{(L/D)}\frac{\Delta P}{\rho U^2} \tag{9}$$

where U is the mean velocity of air.
Thermo-physical property values of air are obtained at the overall bulk air temperature (T_b) in Eq. (3).
Thermal enhancement factor (TEF) is given by

$$\mathrm{TEF} = \left(\frac{\mathrm{Nu}}{\mathrm{Nu}_0}\right)\left(\frac{f}{f_0}\right)^{-1/3} \tag{10}$$

where Nu_0 and f_0 are defined for the plain tube while Nu and f stand for the tube insert.

4. Results and Discussion

4.1 Verification of plain tube

In comparison, Nu and f from the present plain tube and those from the correlations in previous work [17], Dittus-Boelter correlation (Eq. 11) for Nu and Petukhov correlation (Eq. 12) for f, are plotted against each other as presented in Figs. 3(a) and (b), respectively. In the figure, the results from the measured are in good agreement with those from the published correlations. The average deviations of both the results are within ±5.2% and 6.7% for Nu and f, respectively.

Correlation of Dittus and Boelter for heating

$$\mathrm{Nu} = 0.023\mathrm{Re}^{0.8}\mathrm{Pr}^{0.4} \tag{11}$$

Correlation of Petukhov:

$$f = (0.79\ln \mathrm{Re} - 1.64)^{-2} \tag{12}$$

4.2 Heat transfer

The influences of varying R_B and R_P of the DRs on Nu and the augmented Nu or $\mathrm{Nu}/\mathrm{Nu}_0$ are, respectively, depicted in Figs. 4(a) and (b). From Fig. 4(a), Nu values of all inserted tubes increase considerably with rising Re. Obviously, Nu of the DR is considerably higher than the smooth tube alone and shows the uptrend with rising R_B but with the decline of R_P. This can be explained from the fact that the appearance of DRs assists to produce the vortex/swirl flow along the tube, aside from increasing a high turbulence level. The DR at large R_B gives rise to higher blockage of flow, hence, resulting in stronger strength of vortex flow than the one at small value. It is found that the DR possesses Nu around 68–76% over the plain tube and gives the highest Nu of about 76% above the smooth/plain tube with R_B=0.2 and R_P= 0.5.

The variation of $\mathrm{Nu}/\mathrm{Nu}_0$ for using the 45° DR insert with Re is depicted in Fig. 4(b). In the figure, the general tendency of $\mathrm{Nu}/\mathrm{Nu}_0$ for the DR is seen to decrease slightly as Re increases. $\mathrm{Nu}/\mathrm{Nu}_0$ shows the uptrend with increasing R_B but with decreasing R_P. At R_B = 0.2, 0.15 and 0.1, the mean values of $\mathrm{Nu}/\mathrm{Nu}_0$ are respectively, about 4.08, 3.97 and 3.83; 3.91, 3.77 and 3.67; and 3.56, 3.43 and 3.29 times for R_P = 0.5, 1.0 and 2.0. This implies that using the larger R_B and smaller R_P causes a significantly strong flow-circulation aside from more intensity of turbulence and interruption of the boundary layer, leading to the rise in heat transfer. Nonetheless, at this condition, it comes together with substantially higher friction loss, as being seen in the next section.

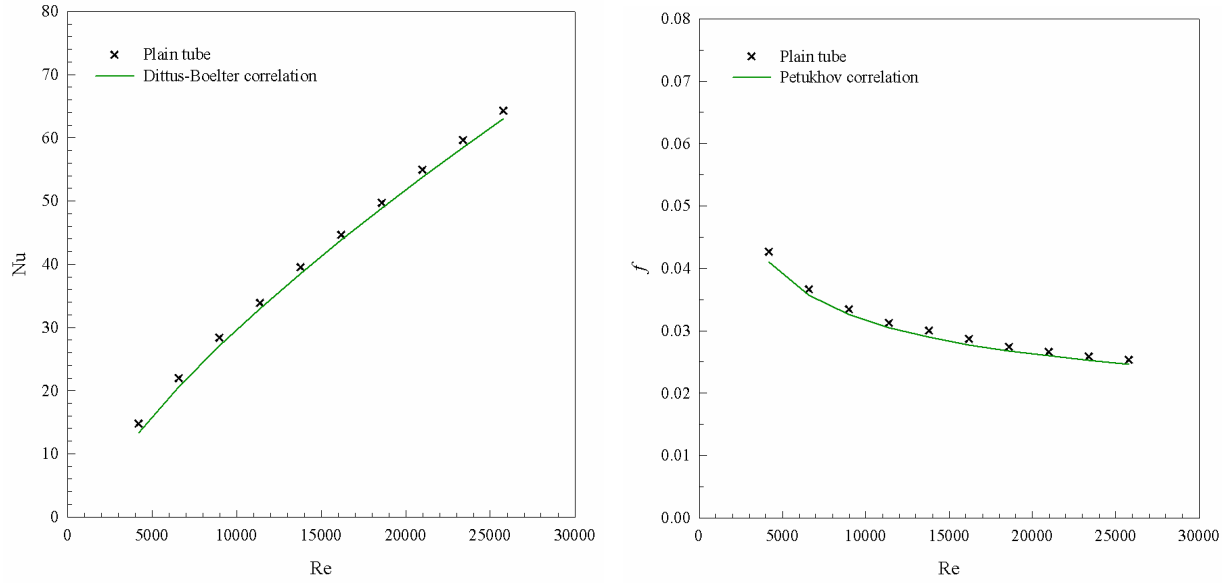

(a) (b)

Fig. 3. Comparison of measured (a) Nu and (b) *f* with published data for the plain tube.

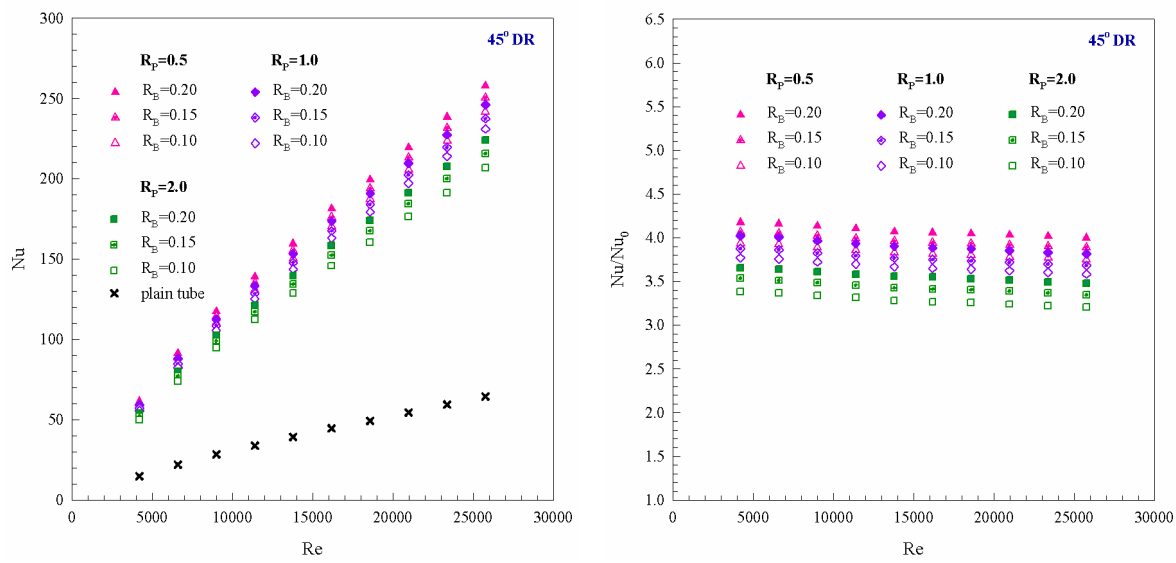

(a) (b)

Fig. 4. Relationships of (a) Nu and (b) Nu/Nu_0 with Re for DRs.

4.3 Flow resistance

The plots of friction factor (*f*) and friction factor ratio (f/f_0) against Re for various R_B and R_P values are, respectively, portrayed in Figs. 5(a) and (b). It can be noted in Fig. 5(a) that the DR yields much higher *f* value above the plain tube and its trend displays a slight decrease with rising Re. A closer examination reveals that *f* tends to rise with the increment in R_B while shows the reversing trend with increasing R_P. This is due to higher flow obstruction, the fluid-viscous dissipation from the increased surface area and the drag by the longitudinal vortex flow, leading to higher flow friction and form drag, especially for large R_B and small R_P. In comparison with the smooth/plain tube, *f* of the DR is increased around 11.73–32.85 times.

As illustrated in Fig. 5(b), it is seen that f/f_0 has the up tendency with rising Re. The employ of DRs gives an extreme increase of f/f_0 with rising Re. It is obvious that f/f_0 shows the uptrend with increasing R_B while exhibits the

reversing trend with rising R_P. The average f/f_0 values for R_B = 0.2, 0.15 and 0.1 are, respectively, about 28.19, 25.04 and 21.85; 22.54, 19.70 and 17.50; and 20.55, 17.83 and 15.19 at R_P = 0.5, 1.0 and 2.0.

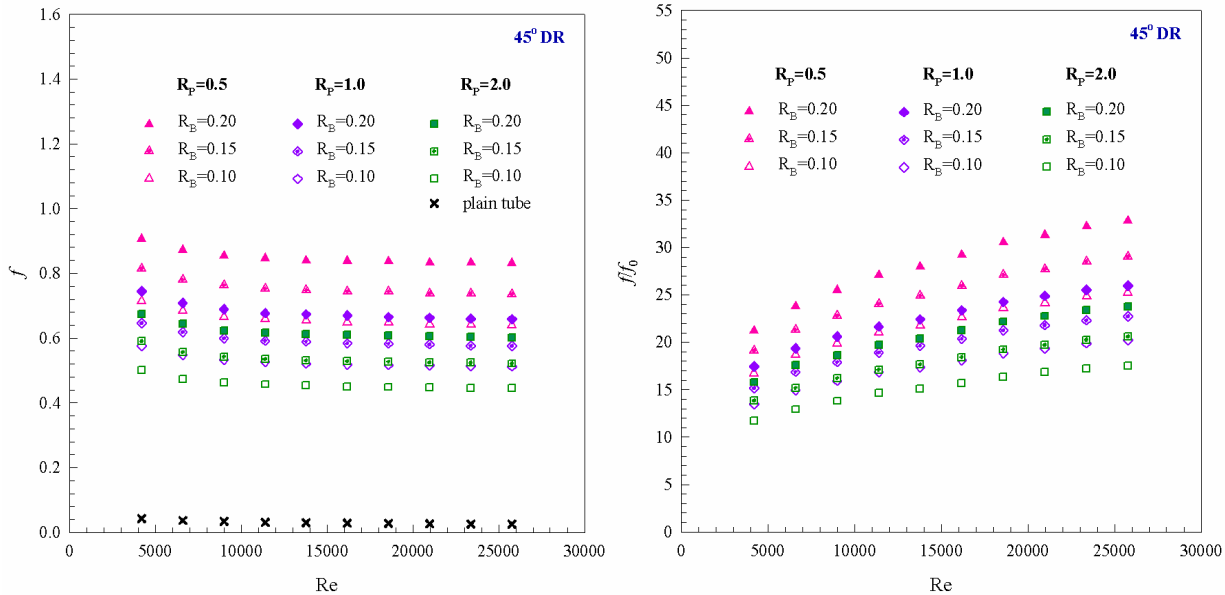

Fig. 5. (a) f and (b) f/f_0 versus Re for DRs.

4.4 Thermal performance

The potentiality of DRs in practical can be assessed via an indicator in terms of thermal enhancement factor (TEF) as denoted in Eq. (10). This result is directly pertinent to the trade-off of the enhanced Nu with the increased f penalty. TEF plotted against Re at different R_B and R_P values is shown in Fig. 6. As seen, all values of TEF are above unity, implying the advantage of the DR over the plain tube alone. TEF shows the down tendency with the rise in Re for DR inserts while the maximum around 1.57 is seen at R_B = 0.1, R_P = 1.0. Also, it is observed that the highest TEF values are in the range of 1.46 to 1.57 for different R_B and R_P values at the lowest Re. Therefore, the best choice of this DR roughness is at R_B = 0.1 and R_P = 1.0 to achieve the superior thermal performance.

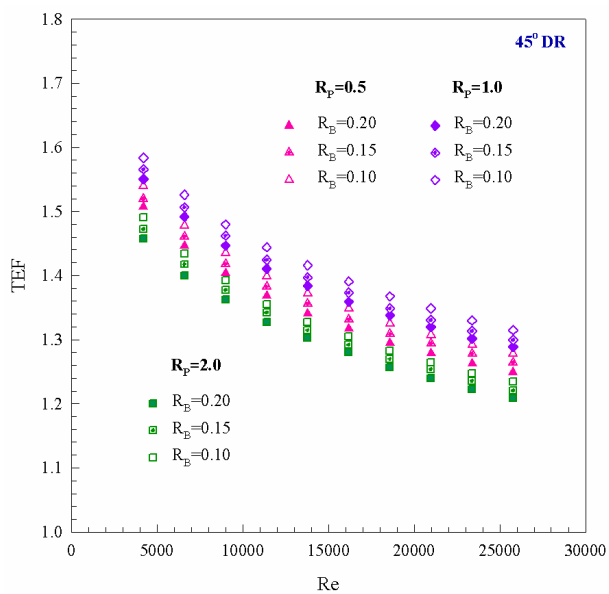

Fig. 6. Variation of TEF with Re for various DRs.

5. EMPIRICAL CORRELATIONS

Empirical correlations of Nu, *f* and TEF for using the 45° DR are determined from the measured data and they are correlated as given in equations (13) – (15). The correlation of Nu is displayed as the function of Re, R_P, R_B and Prandtl number (Pr) whereas *f* and TEF are independent of Pr value. The Nu, *f* and TEF correlations are as follows:

$$Nu = 0.119Re^{0.782}Pr^{0.4}R_B^{0.098}R_P^{-0.072} \tag{13}$$

$$f = 1.891Re^{-0.035}R_B^{0.386}R_P^{-0.16} \tag{14}$$

$$TEF = 3.363Re^{-0.102}R_B^{-0.031}R_P^{-0.019} \tag{15}$$

The reliability of the correlations was tested by plotting the values of Nu, *f* and TEF from the correlations with the experimental data as shown in Figs. 7(a), (b) and (c) respectively. In the figure, it is found that the discrepancies between the predicted and the measured data lie within ±8%, ±9% and ±5% for Nu, *f* and TEF, respectively.

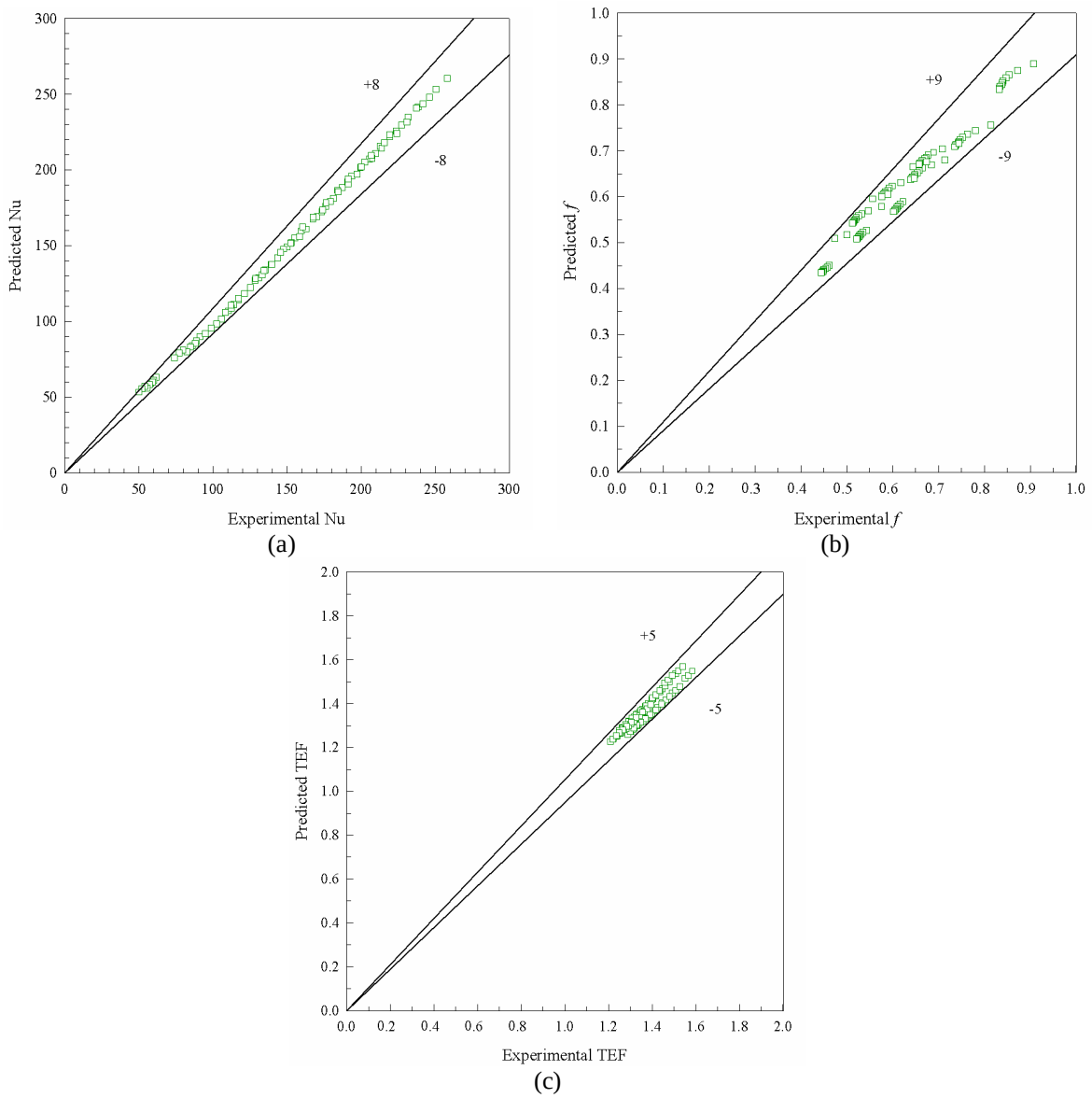

Fig. 7. Comparison of the measured with the predicted (a) Nu, (b) *f* and (c) TEF.

6. CONCLUSIONS

An experimental study of heat transfer and flow resistance behaviors in a tubular heat exchanger with a newly designed vortex ring in the form of diamond-shaped ring (DR) under turbulent flow, Re = 4220–25,800, using air as the test fluid has been conducted. The effects of R_B, R_P and Re on thermal behaviors of the DR inside the tube are investigated. Key findings from the current study are as follows:

1) The use of DR elements yields a significant effect to flow and thermal behaviors in the tube leading to enhancing the heat transfer as well as friction loss.
2) All the DRs provide much higher heat transfer rate than the plain tube alone. The increase in Nu/Nu_0 is ranging from 3.21 to 4.18 times while that in the f/f_0 is around 11.73 to 32.85 times, depending on R_B, R_P and Re.
3) For performance comparison, the highest TEF around 1.57 is at R_B = 0.10 and R_P = 1.0, pointing that in practical, the DR is regarded as a superior device for a tubular heat exchanger.
4) The Nu, *f* and TEF correlations are determined and their values are found to agree well with the measured data. The deviations are within 8%, 9% and 5% for Nu *f*, and TEF, respectively.

NOMENCLATURE

A	[m^2]	heat transfer surface area
e	[m]	height of ring
R_B	[=e/H]	blockage ratio of ring
R_P	[=P/H]	pitch ratio of ring
$C_{p,a}$	[J/kg K]	specific heat of air
D	[m]	tube diameter
f	[-]	friction factor
k	[W/m K]	thermal conductivity of air
$\dot{m}$	[kg/s]	mass flow rate of air
L	[m]	length of test section
Nu	[-]	Nusselt number of roughened duct
P	[m]	pitch length between rings
Q	[W]	heat transfer rate
Pr	[-]	Prandtl number
Re	[-]	Reynolds number
T_i	[^oC]	inlet air temperature
T_o	[^oC]	outlet air temperature
T_b	[^oC]	bulk mean air temperature
TEF	[-]	thermal enhancement factor

Greek symbols

α	[degree]	inclination angle
ν	[N s/m^2]	kinematic viscosity

Subscripts

a	air
w	wall

REFERENCES

[1] Sneha, P., Subrahmanyam T. and Naidu S.V. A comparative study on the thermal performance of water in a circular tube with twisted tapes, perforated twisted tapes and perforated twisted tapes with alternate axis, Int. J. Therm. Sci., Vol. 136, 2019, pp. 530-538.

[2] Keklikcioglu, O. and Ozceyhan, V. Experimental investigation on heat transfer enhancement in a circular tube with equilateral triangle cross sectioned coiled-wire inserts, Appl. Therm. Eng., Vol. 131, 2018, pp. 686-695.

[3] Skullong, S., Promvonge, P., Jayranaiwachira, N. and Thianpong, C. Experimental and numerical heat transfer investigation in a tubular heat exchanger with delta-wing tape inserts, Chem. Eng. Process. Process Intensif., Vol. 109, 2016, pp. 164-177.

[4] Suwannapan, S., Skullong, S. and Promvonge, P. Thermal characteristics in a heat exchanger tube fitted with zigzag-winglet perforated-tapes, J. Res. Appl. Mech. Eng., Vol. 3, 2015, pp. 29-36.
[5] Skullong, S., Promvonge, P., Thianpong, C. and Pimsarn, M. Heat transfer and turbulent flow friction in a round tube with staggered-winglet perforated-tapes, Int. J. Heat Mass Transf., Vol. 95, 2016, pp. 230-242.
[6] Promvonge, P., Koolnapadol, N., Pimsarn, M. and Thianpong, C. Thermal performance enhancement in a heat exchanger tube fitted with inclined vortex rings, Appl. Therm. Eng., Vol. 62, 2014, pp. 285-292.
[7] Chingtuaythong, W., Promvonge, P., Thianpong, C. and Pimsarn, M. Heat transfer characterization in a tubular heat exchanger with V-shaped rings, Appl. Therm. Eng., Vol. 110, 2017, 1164-1171.
[8] Promvonge, P. Thermal performance in circular tube fitted with coiled square wires, Energy Convers. Manage., Vol. 49, 2008, pp. 980-987.
[9] Chiu, Y.W. and Jang, J.Y. 3D numerical and experimental analysis for thermal–hydraulic characteristics of air flow inside a circular tube with different tube inserts, Appl. Therm. Eng., Vol. 29, 2009, pp. 250-258.
[10] Promvonge, P., Pethkool, S., Pimsarn, M. and Thianpong, C. Heat transfer augmentation in a helical-ribbed tube with double twisted tape inserts, Int. Commun. Heat Mass Transf., Vol. 39, 2012, pp. 953-959.
[11] Hong, Y., Du, J. and Wang, S. Turbulent thermal, fluid flow and thermodynamic characteristics in a plain tube fitted with overlapped multiple twisted tapes, Int. J. Heat Mass Transf., Vol. 115, 2017, pp. 551-565.
[12] Man, C., Lv, X., Hu, J., Sun, P. and Tang, Y. Experimental study on effect of heat transfer enhancement for single-phase forced convective flow with twisted tape inserts, Int. J. Heat Mass Transf., Vol. 106, 2017, pp. 877-883.
[13] Kongkaitpaiboon, V., Nanan, K. and Eiamsa-ard, S. Experimental investigation of convective heat transfer and pressure loss in a round tube fitted with circular-ring turbulators, Int. Commun. Heat Mass Transf., Vol. 37, 2010, pp. 568-574.
[14] Promvonge, P., Tamna, S., Pimsarn, M. and Thianpong, C. Thermal characterization in a circular tube fitted with inclined horseshoe baffles, Appl. Therm. Eng., Vol. 75, 2015, pp. 1147-1155.
[15] Skullong, S., Promvonge, P., Thianpong, C., Jayranaiwachira, N. and Pimsarn, M. Thermal performance of heat exchanger tube inserted with curved-winglet tapes, Appl. Therm. Eng., Vol. 129, 2018, pp. 1197-1211.
[16] ANSI/ASME, Measurement uncertainty, PTC 19.1-1985, Part I, 1986, ASME, New York.
[17] Skullong, S., Promvonge, P., Thianpong, C., Jayranaiwachira, N., Pimsarn, M. Heat transfer augmentation in a solar air heater channel with combined winglets and wavy grooves on absorber plate, Appl. Therm. Eng., Vol. 122, 2017, pp. 268-284.
[18] Incropera, F. and Dewitt, P.D. Fundamentals of heat and mass transfer, 6th edition, 2007, Wiley, USA.